The Astrophysical Journal Letters, 962:L26 (6pp), 2024 February 20 https://doi.org/10.3847/2041-8213/ad2466

True Pair-instability Supernova Descendant: Implications for the First Stars' Mass Distribution

Ioanna Koutsouridou[1,2], Stefania Salvadori[1,2], and Ása Skúladóttir[1,2]
[1] Dipartimento di Fisica e Astronomia, Universitá degli Studi di Firenze, Largo E. Fermi 1, 50125, Firenze, Italy; ioanna.koutsouridou@unifi.it
[2] INAF/Osservatorio Astrofisico di Arcetri, Largo E. Fermi 5, 50125, Firenze, Italy
Received 2023 December 8; revised 2024 January 18; accepted 2024 January 31; published 2024 February 13

Abstract

The initial mass function (IMF) of the first Population III (Pop III) stars remains a persistent mystery. Their predicted massive nature implies the existence of stars exploding as pair-instability supernovae (PISNe), but no observational evidence had been found. Now, the LAMOST survey claims to have discovered a pure PISN descendant, J1010+2358, at $[Fe/H] = -2.4$. Here we confirm that a massive 250–260 $M_\odot$ PISN is needed to reproduce the abundance pattern of J1010+2358. However, the PISN contribution can be as low as 10%, since key elements are missing to discriminate between scenarios. We investigate the implications of this discovery for the Pop III IMF, by statistical comparison with the predictions of our cosmological galaxy formation model, NEFERTITI. First, we show that the nondetection of mono-enriched PISN descendants at $[Fe/H] < -2.5$ allows us to exclude (i) a flat IMF at a 90% confidence level; and (ii) a Larson-type IMF with characteristic mass $m_{ch}/M_\odot > 191.16x - 132.44$, where x is the slope, at a 75% confidence level. Second, we show that if J1010+2358 has only inherited <70% of its metals from a massive PISN, no further constraints can be put on the Pop III IMF. If, instead, J1010+2358 will be confirmed to be a nearly pure (>90%) PISN descendant, it will offer strong and complementary constraints on the Pop III IMF, excluding the steepest and bottom-heaviest IMFs: $m_{ch}/M_\odot < 143.21x - 225.94$. Our work shows that even a single detection of a pure PISN descendant can be crucial to our understanding of the mass distribution of the first stars.

Unified Astronomy Thesaurus concepts: Population III stars (1285); Milky Way evolution (1052); Galaxy evolution (594); Galaxy formation (595); Milky Way formation (1053); Theoretical models (2107); Milky Way stellar halo (1060)

1. Introduction

The first Population III (Pop III) stars formed out of primordial composition gas and thus were likely more massive than those observed today, with a mass range possibly extending up to ≈1000 $M_\odot$ (e.g., Hirano et al. 2015). These theoretical findings have strong physical grounds and have been supported across decades by both analytical calculations (e.g., McKee & Tan 2008) and numerical simulations (e.g., Susa et al. 2014). Furthermore, in recent years, stellar archeology has provided novel data-driven constraints on the properties of the first stars, which confirm their massive nature (e.g., Hartwig et al. 2018; Rossi et al. 2021; Koutsouridou et al. 2023). However, the initial mass function (IMF) of the first stars is largely unknown and it is still unclear if primordial stars with hundreds of solar masses were really able to form (e.g., Klessen 2019, for a recent review).

Very massive first stars, $140\,M_\odot \leqslant m_\star \leqslant 260\,M_\odot$, are predicted to end their lives as energetic pair-instability supernovae (PISNe), which completely destroy the progenitor star, injecting into the interstellar medium (ISM) ≈50% of their mass in the form of heavy elements. Stellar evolution calculations for PISNe are very robust (M. Limongi 2023, private communication) and predict the gas to be imprinted with a *unique* chemical signature, showing a strong odd–even effect (Heger & Woosley 2002; Takahashi et al. 2018). PISN descendants, i.e., long-lived stars formed in gaseous environments predominantly imprinted by PISNe, can potentially be found in the most ancient component of our Milky Way (MW) and its dwarf galaxy satellites. They are, however, predicted to be extremely rare, with a metallicity distribution function peaking at $[Fe/H] \approx -2.0$ (e.g., Karlsson et al. 2008; de Bennassuti et al. 2017).

After decades of dedicated searches (e.g., Beers & Christlieb 2005; Aoki et al. 2014; Caffau et al. 2023) and development of novel techniques to pinpoint PISN descendants (Salvadori et al. 2019; Aguado et al. 2023), in 2023 June a remarkable Galactic halo star with very strong odd–even effects has finally been identified by the LAMOST survey (Xing et al. 2023). This very metal-poor (VMP) star, J1010+2358, has $[Fe/H] \approx -2.42 \pm 0.12$, and exhibits extremely low abundances of odd elements such as Na and Sc. Furthermore, it shows very large abundance variance between the odd and even elements, such as [Na/Mg] and [Co/Ni]. Thus, Xing et al. (2023) claimed it to be a "pure descendant" of a very energetic PISN progenitor with a mass of 260 $M_\odot$.

Ultimately, despite the identification of stars that might have been partially imprinted by PISNe (Aoki et al. 2014; Salvadori et al. 2019; Aguado et al. 2023; Caffau et al. 2023), J1010+2358 represents so far the unique candidate of a pure PISN descendant. But is the abundance pattern of J1010+2358 only consistent with mono-enrichment by a single 260 $M_\odot$ PISN, or do other solutions exist? What are the implications of the detection of a single PISN descendant with $[Fe/H] \approx -2.5$ for the IMF of the first stars? The aim of this Letter is to address these questions by comparing the observed frequency of PISN

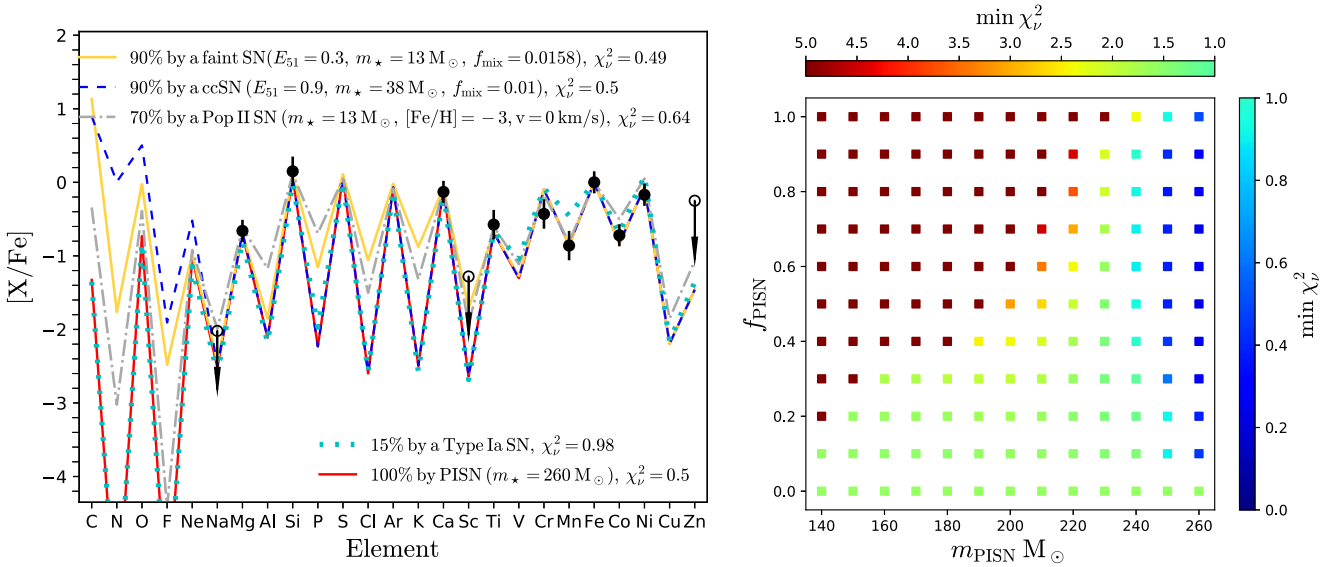

Figure 1. Left: measured chemical abundances of J1010+2358 (black points with errorbars) compared to (i) a 260 $M_\odot$ PISN (red); (ii) 10% of metals by a 260 $M_\odot$ PISN and 90% by a primordial faint SN (yellow) or a primordial core-collapse SN (blue; yields by Heger & Woosley 2010); (iii) 30% of metals by a massive PISN and 70% by a Population II SN (gray; Limongi & Chieffi 2018); (iv) 85% of metals by a massive PISN and 15% by a Type Ia SN (cyan; model W70 by Iwamoto 1999). Right: minimum χ^2_ν of the fit to J1010+2358's chemical abundances with different fractions of PISN enrichment, $f_{\rm PISN}$, from a mass $m_{\rm PISN}$ progenitor, and the rest from Pop III SNe.

descendants with predictions from state-of-the-art cosmological models for the MW formation.

2. Observations: PISN Descendants

To discriminate among model predictions that assume different Pop III IMFs, we should quantify the observed frequency of PISN descendants. However, we first need to clarify whether J1010+2358 has truly been mono-enriched by a single 260 $M_\odot$ PISN or if other enrichment channels are also possible.

2.1. Is J1010+2358 Mono-enriched by a PISN?

In Figure 1 (left) we see that the observed abundance pattern[3] of J1010+2358 is in perfect agreement with the one predicted for a pure enrichment by a 260 $M_\odot$ PISN, as stated by Xing et al. (2023). The fit of the model to the observed data is extremely good, $\chi^2_\nu=\chi^2/\nu=0.5$, where ν is the total number of observed data points, including normal (N) measurements, upper (U) and lower (L) limits, and

$$\chi^2=\sum_{i=1}^{N}\frac{(F_i-D_i)^2}{\sigma_i^2}+\sum_{i=N+1}^{N+U+L}\frac{(F_i-D_i)^2}{\sigma_i^2}\Theta(F_i-D_i), \quad (1)$$

following Heger & Woosley (2010). Here, F_i and D_i are the theoretical and observed values of [X/Fe], respectively, σ_i are the observational uncertainties, and $\Theta(x)=1$ for $x>0$ ($x<0$) if D_i is an upper (lower) limit, and $x=0$ otherwise.

To understand whether J1010+2358 could also be "multi-enriched," we analyze the simplest case, that is an enrichment by two different supernovae (SNe). We assume that a fraction $f_{\rm PISN}$ of its metals has been contributed by a PISN with mass $m_{\rm PISN}=$ [140–260] $M_\odot$, while the remainder comes from a second SN, which can be of any other type: a Pop III SN (ranging in energy, mixing, and mass) or a Pop II SN (ranging in mass and metallicity), thus more generally named SN$_j$. The chemical abundance pattern of a star imprinted by these two SNe would be

$$F_i=[\mathrm{X/Fe}]=\log\left(\frac{\mathrm{Y}_X^{\rm PISN}+\beta\frac{\mathrm{Y}_Z^{\rm PISN}}{\mathrm{Y}_Z^{\rm SN_j}}\mathrm{Y}_X^{\rm SN_j}}{\mathrm{Y}_{Fe}^{\rm PISN}+\beta\frac{\mathrm{Y}_Z^{\rm PISN}}{\mathrm{Y}_Z^{\rm SN_j}}\mathrm{Y}_{\rm Fe}^{\rm SN_j}}\right)+ -\log\left(\frac{\mathrm{M}_X}{\mathrm{M}_{Fe}}\right)_\odot \quad (2)$$

(Salvadori et al. 2019), where $\beta=(1-f_{\rm PISN})/f_{\rm PISN}$, $\mathrm{Y_X}^{\rm PISN}$, $\mathrm{Y}_X{}^{\rm SN_j}$ are the theoretical elemental yields and $\mathrm{Y_Z}^{\rm PISN}$, $\mathrm{Y_Z}^{\rm SN_j}$ the total metal yields of the PISN and SN$_j$, respectively (see the caption of Figure 1 for the adopted yields). By substituting the above in Equation (1), we determine the best fit over all SN$_j$ (minimum χ^2_ν) to the abundance pattern of J1010+2358, for each $f_{\rm PISN}$ and $m_{\rm PISN}$.

The results are shown in Figure 1 (right). We find that a contribution from a PISN with 250–260 $M_\odot$ is necessary to reproduce the abundance pattern of J1010+2358: $\chi^2_\nu<1$ for $m_{\rm PISN}\geqslant 250\,M_\odot$ and $f_{\rm PISN}\geqslant 0.1$. The goodness of fit in each case depends on the properties of the secondary SN. Even for $f_{\rm PISN}=0.1$, there exist numerous Pop III SNe of different type j that can yield $\chi^2_\nu\leqslant 1$. Two such examples are shown in the left panel of Figure 1. When Pop II SNe are investigated, we find that a minimum contribution of $f_{\rm PISN}=0.3$ is required to match J1010+2358's abundance pattern (Figure 1, gray line). As in the case of Pop III SNe, the massive PISN contribution here is necessary to reproduce the observed strong odd–even effect or/and the low [Na/Fe] and [Sc/Fe] ratios. Furthermore, $\chi^2_\nu<1$ only when the contribution from Type Ia SNe is <15% (Figure 1, cyan line). Otherwise, the iron-peak elements Mn, Ni, and Co are overrepresented against the lighter elements Mg and Si. Nevertheless, the contribution of Type Ia SNe to second-generation stars is likely minimal due to their typical delay times (Komiya & Shigeyama 2016).

[3] For Ti, we use the average of the Ti I and Ti II measurements, which have a difference of 0.15 dex.

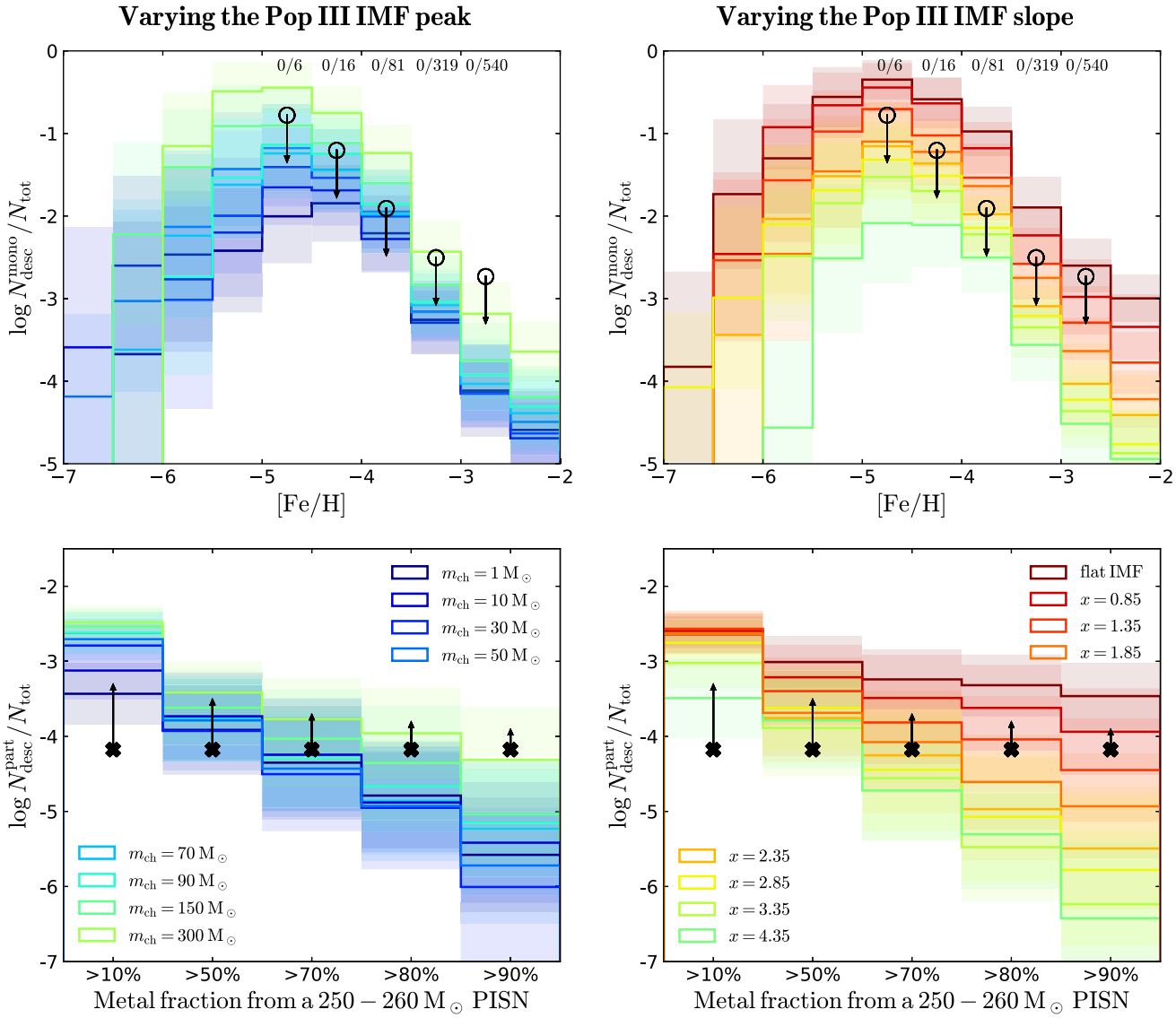

Figure 2. Top: predicted fraction of mono-enriched PISN descendants in the inner halo as a function of [Fe/H], when varying the characteristic mass of the Pop III IMF, for $x = 2.35$ (left); and when varying x, for $m_{\rm ch} = 70\,M_\odot$ (right; Equation (3)). A Gaussian error of 0.2 dex has been applied to model predictions to account for observational uncertainties. Data points show the observed fractions (Section 2.2), also listed on top. Bottom: predicted fraction of all [Fe/H] $\leqslant -2$ inner halo stars that have inherited at least 10%, 50%, 70%, 80%, or 90% of their metals from a 250 to 260 $M_\odot$ PISN, for different $m_{\rm ch}$ (left) and slope x (right) of the Pop III IMF. The X mark denotes that *at least* one star, J1010+2358, out of 15,000 VMP stars in the LAMOST sample has been imprinted by a 250–260 $M_\odot$ PISN (Section 2.1). Histograms and shaded areas represent the mean and standard deviation of 200 runs of each model.

These results indicate that J1010+2358 could be imprinted by a 250–260 $M_\odot$ PISN and one or multiple SNe. Alternatively, there exists the possibility that J1010+2358 has been completely enriched by peculiar 12–14 $M_\odot$ core-collapse SNe that experience negligible fallback (Jeena et al. 2024).

2.2. Frequency of Mono-enriched PISN Descendants

The star J1010+2358 is VMP ([Fe/H] $\leqslant -2$) with subsolar [Mg/Fe] based on the low-resolution LAMOST survey (Zhao et al. 2012), which comprises over 15,000 VMP stars (Aoki et al. 2022; Li et al. 2022). J1010+2358 was followed up at high resolution and confirmed as a probable PISN descendant (Xing et al. 2023). Since only a small subset of the LAMOST sample has been followed up at high resolution, more of these stars could possibly harbor an imprint from a 250 to 260 $M_\odot$ PISN. Therefore, we can treat the identified fraction of massive PISN descendants, $\sim$1/15,000, as a lower limit to compare with our theoretical predictions (Figure 2, bottom).

Using the SAGA[4] database (e.g., Suda et al. 2008, 2017), we examine whether more VMP stars have abundance patterns consistent with mono-enrichment by a PISN. Searching for a partial PISN enrichment would be inconclusive, since contribution from other SNe can mask the distinctive PISNe signature. We restrict our analysis to Galactic halo stars with at least six elemental abundance measurements (excluding upper limits), and excluding CEMP-s stars, since their abundance patters are not representative of their birth environments. In case of multiple entries from different surveys/authors for the same star, we keep the one with the most measured abundances. We end up with a sample of 962 unique stars with $-5 \leqslant$ [Fe/H] < -2.5.

[4] http://sagadatabase.jp/

Most chemical abundances in our sample have been measured assuming a one-dimensional, local thermodynamic equilibrium (LTE) hydrostatic model atmosphere. Following Ishigaki et al. (2018), we thus assign a large observational uncertainty of 0.3 dex to the abundances of C, N, O, Na and Al that are strongly affected by non-LTE effects. Additionally, we adopt a 0.2 dex error for Si, Ti, Cr, and Mn because their measured abundances vary significantly depending on the absorption lines used to derive them. For all other elements, we assume a 0.15 dex error, unless a larger uncertainty is reported in the literature. Due to the large errors assumed, we require that $\chi^2_\nu \leqslant 1$ for a fit to be considered good.

As expected, zero stars from the SAGA sample at $[\mathrm{Fe/H}] < -2.5$ are consistent with enrichment by a single PISN progenitor. We use this nondetection to adopt upper limits on the fraction of mono-enriched PISN descendants (Figure 2, top).

3. Theory: Summary of NEFERTITI

The code NEFERTITI (NEar FiEld cosmology: Re-Tracing Invisible TImes; details in Koutsouridou et al. 2023), is a state-of-the-art cosmological chemical evolution model intended to study the unknown properties of the first stars (IMF and energy distribution of the first SNe). NEFERTITI can run on halo merger trees obtained from *N*-body cosmological simulations or Monte Carlo techniques, and grounds on previous semianalytical models for the Local Group formation (Salvadori et al. 2007, 2015; Pagnini et al. 2023). Here we employ NEFERTITI coupled with a cold dark matter (DM) *N*-body simulation of an MW analog (fully described in Koutsouridou et al. 2023), which successfully reproduces the present-day global properties of the MW (metallicity and mass of both stars and gas) and the metallicity distribution function of the Galactic halo (Bonifacio et al. 2021). In the following, we recap the main assumptions and innovative aspects of the semianalytical model.

NEFERTITI follows the evolution of the baryonic component within DM halos based on the following assumptions: (i) at the highest redshift of the simulation the intergalactic medium (IGM) has a primordial composition; (ii) gas from the IGM is continuously accreted onto each halo at a rate proportional to the halo's DM growth and subsequently streams onto the halo's central galaxy in freefall; (iii) stars form in DM halos that exceed a minimum mass, which evolves through cosmic times to account for the photodissociating and ionizing radiation (Salvadori & Ferrara 2009); (iv) within each galaxy, stars form on a rate proportional to the available gas mass, the rate being reduced in minihalos (with virial temperature $T_{\rm vir} \leqslant 2 \times 10^4$ K) to account for the ineffective cooling by molecular hydrogen (Salvadori & Ferrara 2012); (v) gas and metals that are returned through stellar winds and SNe to the ISM and the IGM are assumed to be instantaneously mixed; (vi) at each time step, the stellar, gas and metal masses within each DM halo are equally distributed among its particles and remain attached to them to the next integration step.

The most innovative aspects of NEFERTITI are that the code accounts for the

1. incomplete sampling of the stellar IMF (Rossi et al. 2021) for Pop III and Pop II/I stars;
2. unknown Pop III IMF, parameterized as (Larson 1998)

$$\phi(m_\star) = \frac{dN}{dm_\star} \propto m_\star^{-x} \exp\left(-\frac{m_{\rm ch}}{m_\star}\right), \quad (3)$$

   where $m_\star = [0.8\text{–}1000]\, M_\odot$ following Rossi et al. (2021), and the characteristic mass, $m_{\rm ch}$, and IMF slope, x, are varied; while normal Pop II/I stars form according to a Larson IMF with $m_{\rm ch} = 0.35\, M_\odot$, $x = 2.35$, and $m_\star = [0.1\text{–}100]\, M_\odot$ when the ISM has a metallicity $Z \geqslant Z_{\rm crit} = 10^{-4.5}\, Z_\odot$ (de Bennassuti et al. 2017);
3. evolution of individual stars in their proper timescales, adopting the yields of Heger & Woosley (2002, 2010) for Pop III stars and Van Den Hoek & Groenewegen (1997) and Limongi & Chieffi (2018) for Pop II/I stars;
4. unknown energy distribution function of the Pop III SNe ($m_\star = [10\text{–}100]\, M_\odot$), parameterized as $\mathrm{d}N/\mathrm{d}E \propto E_\star^{-\alpha_e}$, where α_e can be varied. Here we adopt $\alpha_e = 2$.

In star-forming minihalos, the available star-forming gas is sometimes less than the maximum stellar mass permitted by our assumed IMF, prohibiting the formation of massive stars and skewing the effective IMF toward low masses. Here, we use the following approach to adhere to our assumed IMF without favoring multienrichment. Whenever the random mass generator calls for the formation of a star whose mass exceeds the available star-forming gas mass, we postpone star formation in that halo until enough gas accumulates to allow that massive star's formation.

4. Results

We can now try to constrain the Pop III IMF through two key comparisons: (i) the fraction of mono-enriched PISN descendants with $[\mathrm{Fe/H}] < -2.5$ predicted to lie in the inner Galactic halo (Galactocentric radii $7\ \mathrm{kpc} \leqslant R_{\rm gal} \leqslant 20\ \mathrm{kpc}$) at $z = 0$, contrasting this with their absence in the SAGA database (Figure 2, top); (ii) the predicted fraction of VMP stars that have been enriched by a massive 250–260 $M_\odot$ PISN progenitor, in relation to the unique star so far identified with these properties, J1010+2358 (Figure 2, bottom). For the latter, we consider separately the fraction of stars imprinted at a >10%, >50%, >70%, >80%, and >90% level by their massive PISN progenitor. In each case we assume that at least one star fits the criteria, J1010+2358 (Section 2.1).

Figure 2 shows our results when varying the characteristic mass of the Pop III IMF (Equation (3)) for a constant slope $x = 2.35$ (left panels), and the slope x for a characteristic mass $m_{\rm ch} = 70\, M_\odot$ (right panels). We find that a number of mono-enriched PISN descendants survive in the Galactic halo, spanning $[\mathrm{Fe/H}] < -5$ up to at least $[\mathrm{Fe/H}] = -2$ (Figure 2, top panels; see also Magg et al. 2022). In all cases, the predicted fractions show a maximum at $-5 \leqslant [\mathrm{Fe/H}] \leqslant -4.5$. At lower metallicities, the fraction decreases, since only the lowest-mass PISNe ($m_{\rm PISN} < 150\, M_\odot$) produce such little iron to result in $[\mathrm{Fe/H}]_{\rm ISM} < -5$ (Salvadori et al. 2019). At $[\mathrm{Fe/H}] > -4.5$, the fraction of mono-enriched PISN descendants decreases strongly again, because of the gradual dominance of stars mainly imprinted by normal Pop II SNe (Figures 7–8 in Koutsouridou et al. 2023).

We find that the expected fraction of both partially and mono-enriched PISN descendants increases both with increasing $m_{\rm ch}$ and when the IMF gets flatter (decreasing x), naturally, since in these cases more PISNe are formed. From Figure 2

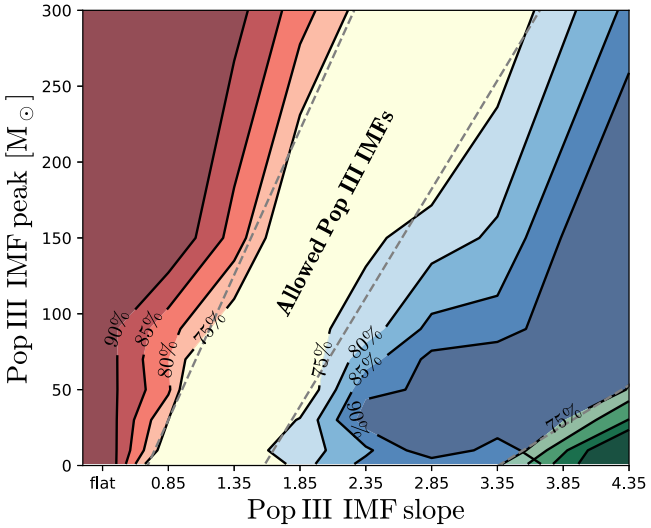

Figure 3. Confidence levels at which we can exclude a Pop III IMF with characteristic mass $m_{\rm ch}$ and slope x, based on (i) the nondetection of mono-enriched PISNe descendants in the SAGA catalog at [Fe/H] < -2.5 (top-left; red contours), and (ii) the discovery of J1010+2358 among 15000 VMP LAMOST stars (bottom-right), assuming that J1010+2358 has inherited >70% (green contours) or >90% (blue contours) of its metals from a 250 to 260 $M_\odot$ PISN. Dashed lines show linear fits to the 75% confidence levels. The central, light-yellow area represents Pop III IMFs that remain possible.

(top), it seems like certain models are disfavored, e.g., $m_{\rm ch} = 300\,M_\odot$, since they suggest that some mono-enriched PISN descendants should have already been identified at [Fe/H] < -2.5. However, to limit the Pop III IMF, it is necessary to quantify the confidence level of the exclusion and to explore the entire parameter space (Figure 3).

In the bottom panels of Figure 2, we focus on the descendants of massive 250–260 $M_\odot$ PISNe, and quantify their predicted fraction, for a given $f_{\rm PISN}$, with respect to the overall stellar population at [Fe/H] $\leqslant -2$. Our predictions are compared to the unique star, J1010+2358, so far identified to be consistent with a minimum 10% enrichment by a massive PISN within the LAMOST VMP stellar sample (Section 2.1). Since other stars partially imprinted by massive PISNe might be present in this sample, we cannot exclude IMFs that lie *above* the observational data point. Therefore, if future observations prove J1010+2358 to be enriched only at a <50% level by a massive PISN, we will not be able to put significant constraints on the Pop III IMF. What if instead J1010+2358 has been predominantly (>50%) enriched by a massive PISN?

For each characteristic mass $m_{\rm ch}$, and Pop III IMF slope x (Equation (3)), we compute the mean probability, P_0, of *not* having detected any mono-enriched PISN descendant among the 962 SAGA stars with [Fe/H] < -2.5, and its statistical error, δP_0, between 200 model realizations:

$$P_0 = \frac{(N_{\rm tot} - N_{\rm desc})!(N_{\rm tot} - N_{\rm obs})!}{N_{\rm tot}!(N_{\rm tot} - N_{\rm desc} - N_{\rm obs})!} \approx \left(1 - \frac{N_{\rm desc}}{N_{\rm tot}}\right)^{N_{\rm obs}}, \quad (4)$$

where $N_{\rm tot}$, $N_{\rm desc}$, and $N_{\rm obs}$ are the total number of expected stars, PISN descendants, and observed stars in each [Fe/H] bin[5] and the approximation is valid for $N_{\rm tot} >> N_{\rm obs}$. The probability of finding *at least* one star enriched by a massive 250–260 $M_\odot$ PISN at a >X% level is given by $1 - P_0 = 1 - \left(1 - \frac{N_{X\%}}{N_{tot}}\right)^{N_{\rm obs}}$, using the above equation. If one of these two probabilities result in $\mathrm{P} + \delta\mathrm{P} < 0.25$, then we can exclude the assumed Pop III IMF with a confidence level of $[1 - (\mathrm{P} + \delta\mathrm{P})] > 75\%$.

Figure 3 illustrates our results. By exploiting the *nondetection* of mono-enriched PISN descendants among the observed stars at [Fe/H] < -2.5, we can already exclude a flat IMF at a >90% confidence level. At a >75% confidence level, we can also exclude Pop III IMFs with characteristic mass $m_{\rm ch}/M_\odot > 191.16x - 132.44$ (leftmost dashed line in Figure 3). If J1010+2358 is found to be enriched at a 70% level by a 250–260 $M_\odot$ PISN, we would only be able to exclude IMFs with $m_{\rm ch}/M_\odot < 53.33x - 179.03$ (rightmost dashed line in Figure 3). If, however, J1010+2358 proves to be enriched >90% by a massive PISN, it would provide much tighter constraints on the Pop III IMF; excluding a Salpeter-like slope ($x = 2.35$) with $m_{\rm ch} \lesssim 130\,M_\odot$, and Pop III IMFs with steeper slopes at a confidence level that increases with increasing x and decreasing $m_{\rm ch}$ (dashed line in Figure 3 corresponding to $m_{\rm ch}/M_\odot = 143.21x - 225.94$ at a 75% confidence level).

5. Discussion and Conclusions

After decades of dedicated searches, the first very promising PISN descendant, J1010+2358, has been discovered within the LAMOST survey (Xing et al. 2023). Here, we have confirmed that a contribution from a massive (250–260 $M_\odot$) PISN is necessary to reproduce its abundance pattern. However, the PISN contribution can be as low as 10% with the rest of its metals coming from other SNe (Figure 1). Exploiting our novel cosmological galaxy formation model of an MW analog, NEFERTITI (Koutsouridou et al. 2023), we investigate the implications for the Pop III IMF of (i) the nondetection of mono-enriched PISN descendants with [Fe/H] < -2.5 in the Galactic halo, and (ii) the discovery of J1010+2358 at [Fe/H] $= -2.4$ (Figure 2).

The nondetection of mono-enriched PISN descendants allows us to exclude at a >90% confidence level a flat Pop III IMF (Figure 3), which has both been favored (e.g., Hirano & Bromm 2017; Parsons et al. 2022) and disfavored (e.g., de Bennassuti et al. 2017) by previous studies. Furthermore, we can exclude at a >75% confidence level, a Larson-type Pop III IMF with characteristic mass $m_{\rm ch}/M_\odot > 191.16x - 132.44$, where x is the slope (Equation (3)). This area rules out the shallower IMFs considered for Pop III stars (e.g., Tarumi et al. 2020; Chen et al. 2022). On the other hand, the constraining power of J1010+2358's discovery, depends on the fraction of its PISN metal enrichment. If >90% of J1010+2358's metals have been inherited from a massive PISN progenitor, then the parameter space of the Pop III IMF can be significantly reduced; where $m_{\rm ch}/M_\odot < 143.21x - 225.94$ is excluded at a 75% confidence level. This rules out Salpeter-like IMFs with $m_{\rm ch} < 130\,M_\odot$ commonly adopted in the literature (e.g., Pallottini et al. 2015; Komiya & Shigeyama 2016; Trinca et al. 2023; Pagnini et al. 2023). If, however, the PISN contribution is only <70%, then the Pop III IMF cannot be further constrained.

Our results are inevitably subject to model assumptions and uncertainties, such as the instantaneous mixing approximation and the adopted stellar yields (see Koutsouridou et al. 2023).

[5] The cumulative probability of *not* observing PISN descendants at [Fe/H] < -2.5 is the product of the probabilities in each bin.

However, they represent a big leap forward in our understanding of the mass distribution of the first stars.

To make further progress, we need to (i) assess the PISN enrichment level of J1010+2358 by measuring additional key elemental abundances such as C, Al, and K (Figure 1); and (ii) significantly increase the number of stars with high-quality spectra. Indeed, here we have shown that even a single detection of a true PISN descendant can dramatically impact our view on the nature of the first stars.

Acknowledgments

We thank the anonymous referee for the useful and constructive comments. This project has received funding from the European Research Council (ERC) under the European Union's Horizon 2020 research and innovation program (grant agreement No. 804240; PI S. Salvadori).

ORCID iDs

Ioanna Koutsouridou https://orcid.org/0000-0002-3524-7172
Stefania Salvadori https://orcid.org/0000-0001-7298-2478
Ása Skúladóttir https://orcid.org/0000-0001-9155-9018

References

Aguado, D. S., Salvadori, S., Skúladóttir, Á, et al. 2023, MNRAS, 520, 866
Aoki, W., Li, H., Matsuno, T., et al. 2022, ApJ, 931, 146
Aoki, W., Tominaga, N., Beers, T. C., Honda, S., & Lee, Y. S. 2014, Sci, 345, 912
Beers, T. C., & Christlieb, N. 2005, ARA&A, 43, 531
Bonifacio, P., Monaco, L., Salvadori, S., et al. 2021, A&A, 651, A79
Caffau, E., Lombardo, L., Mashonkina, L., et al. 2023, MNRAS, 518, 3796
Chen, L.-H., Magg, M., & Hartwig, T. 2022, MNRAS, 513, 934
de Bennassuti, M., Salvadori, S., Schneider, R., Valiante, R., & Omukai, K. 2017, MNRAS, 465, 926
Hartwig, T., Yoshida, N., Magg, M., et al. 2018, MNRAS, 478, 1795
Heger, A., & Woosley, S. E. 2002, ApJ, 567, 532
Heger, A., & Woosley, S. E. 2010, ApJ, 724, 341
Hirano, S., & Bromm, V. 2017, MNRAS, 470, 898
Hirano, S., Hosokawa, T., Yoshida, N., Omukai, K., & Yorke, H. W. 2015, MNRAS, 448, 568
Ishigaki, M. N., Tominaga, N., Kobayashi, C., & Nomoto, K. 2018, ApJ, 857, 46
Iwamoto, K., Brachwitz, F., Nomoto, K., et al. 1999, ApJS, 125, 439
Jeena, S. K., Banerjee, P., & Heger, A. 2024, MNRAS, 527, 4790
Karlsson, T., Johnson, J. L., & Bromm, V. 2008, ApJ, 679, 6
Klessen, R. 2019, in Formation of the First Black Holes, ed. M. Latif & D. Schleicher (Singapore: World Scientific), 67
Komiya, Y., & Shigeyama, T. 2016, ApJ, 830, 76
Koutsouridou, I., Salvadori, S., Skúladóttir, Á., et al. 2023, MNRAS, 525, 190
Larson, R. B. 1998, MNRAS, 301, 569
Li, H., Aoki, W., Matsuno, T., et al. 2022, ApJ, 931, 147
Limongi, M., & Chieffi, A. 2018, ApJS, 237, 13
Magg, M., Schauer, A. T. P., Klessen, R. S., et al. 2022, ApJ, 929, 119
McKee, C. F., & Tan, J. C. 2008, ApJ, 681, 771
Pagnini, G., Salvadori, S., Rossi, M., et al. 2023, MNRAS, 521, 5699
Pallottini, A., Ferrara, A., Pacucci, F., et al. 2015, MNRAS, 453, 2465
Parsons, J., Mas-Ribas, L., Sun, G., et al. 2022, ApJ, 933, 141
Rossi, M., Salvadori, S., & Skúladóttir, Á. 2021, MNRAS, 503, 6026
Salvadori, S., Bonifacio, P., Caffau, E., et al. 2019, MNRAS, 487, 4261
Salvadori, S., & Ferrara, A. 2009, MNRAS, 395, L6
Salvadori, S., & Ferrara, A. 2012, MNRAS, 421, L29
Salvadori, S., Schneider, R., & Ferrara, A. 2007, MNRAS, 381, 647
Salvadori, S., Skúladóttir, Á., & Tolstoy, E. 2015, MNRAS, 454, 1320
Suda, T., Hidaka, J., Aoki, W., et al. 2017, PASJ, 69, 76
Suda, T., Katsuta, Y., Yamada, S., et al. 2008, PASJ, 60, 1159
Susa, H., Hasegawa, K., & Tominaga, N. 2014, ApJ, 792, 32
Takahashi, K., Yoshida, T., & Umeda, H. 2018, ApJ, 857, 111
Tarumi, Y., Hartwig, T., & Magg, M. 2020, ApJ, 897, 58
Trinca, A., Schneider, R., Valiante, R., et al. 2023, arXiv:2305.04944
Van Den Hoek, L., & Groenewegen, M. A. 1997, A&AS, 123, 305
Xing, Q.-F., Zhao, G., Liu, Z.-W., et al. 2023, Natur, 618, 712
Zhao, G., Zhao, Y.-H., Chu, Y.-Q., Jing, Y.-P., & Deng, L.-C. 2012, RAA, 12, 723